

# Grasping without Squeezing: Shear Adhesion Gripper with Fibrillar Thin Film

Elliot W. Hawkes, David L. Christensen, Amy Kyungwon Han, Hao Jiang, and Mark R. Cutkosky

**Abstract**—Nearly all robotic grippers have one trait in common: they grasp objects with normal forces, either directly, or indirectly through friction. This method of grasping is effective for objects small enough for a given gripper to partially encompass. However, to grasp larger objects, significant grip forces and a high coefficient of friction are required. We present a new grasping method for convex objects, using almost exclusively shear forces. We achieve shear grasping with a gripper that utilizes thin film gecko-inspired fibrillar adhesives that conform to the curvature of the object. We present a verified model for grasping a range of curvatures and results that demonstrate the thin film fibrillar adhesives’ increased contact area on textured surfaces when loaded in shear. Finally, the gripper is implemented on a robotic arm and grasps a variety of convex objects (at rest and ballistic).

## I. INTRODUCTION

The last half century has produced countless robotic grippers, ranging from fully actuated, rigid hands [1]–[3] to underactuated, compliant, and back drivable hands [4]–[10]. A summary and literature review is provided in [11]. All of these grippers apply normal forces to grasp an object. The normal forces may either directly support the object through a wrapped grasp, in which case friction is unnecessary (form closure), or squeeze the object to create enough friction for a stable grasp (force closure) [12]. In many cases, some combination of direct support and friction is used. This traditional method of grasping with normal forces is obviously very robust and flexible; it allows robotic as well as human hands to not only grasp a huge range of objects but also dextrously manipulate many of them.

A limitation of traditional normal force grasping arises when an object (here assumed to be spherical for simplicity) is too large for a gripper to wrap at least half way around. The gripper must squeeze the object and utilize friction to hold it. However, larger objects will tend to be squeezed out of the grasp unless the coefficient of friction also increases with the size of the object. The coefficient of friction cannot be increased without limit.

A handful of alternatives to traditional normal force grasping exist. Suction is often used in manufacturing for lifting featureless objects. Particle jamming combined with suction and friction has also been shown to hold objects [13]. A mushroom-tipped adhesive gripper can lift objects after the adhesive is made to stick by pressing it onto an object, and can lift 0.41N, or 2 kPa [14]. These methods use a normal force directed away from the object to lift it.

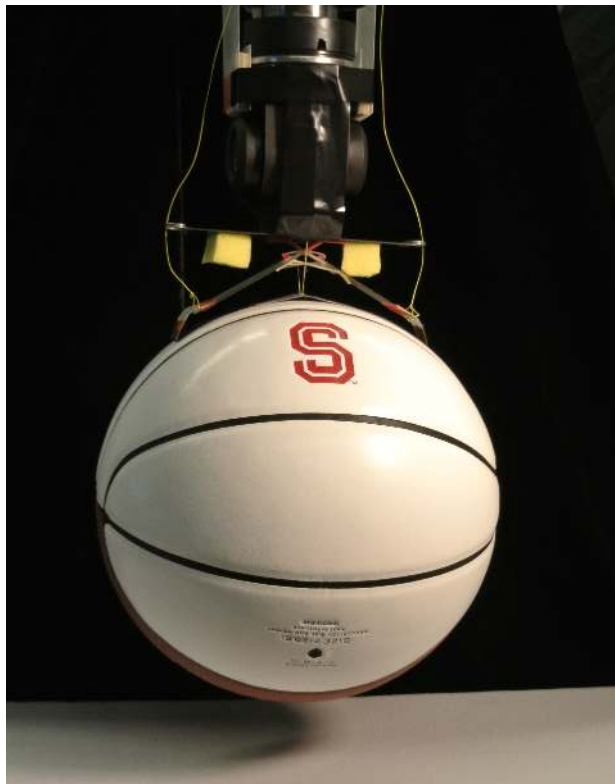


Fig. 1: Shear force gripper holding a regulation-size basketball.

In contrast to all methods mentioned above, we present a new method of grasping that relies on shear adhesion rather than normal forces. Adhesive shear forces are developed along the surface of an object in the directions of the local tangents using controllable fibrillar adhesives. The resultant of these forces holds the object. A shear adhesion gripper can grasp large, relatively featureless convex objects, unlike traditional grippers (Fig. 1). Further, it does not require power or pneumatics like suction solutions, nor does it require the adhesive to be pressed onto the object.

We realize shear adhesion grasping with thin film gecko-inspired dry adhesives which turn on when loaded in shear. The gripper lays 2 (or more) strips of adhesive-coated kapton film onto the object’s surface; these strips self-engage when loaded and require no squeezing. Because no active squeezing is required, the gripper can passively and dynamically grasp objects, i.e. it is able to catch thrown items without active control.

In this paper, we present (1) the design of the shear force

<sup>1</sup>E.W. Hawkes is with the Department of Mechanical Engineering at Stanford University, 450 Serra Mall, Stanford, CA 94305, USA ewhawkes at stanford.edu

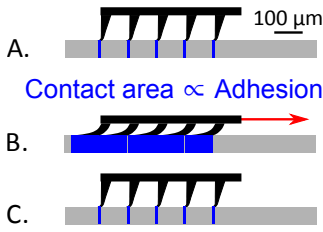


Fig. 2: A) Bringing the microwedge adhesive within a few microns of a surface allows the tips of the wedges to engage with the surface. B) When loaded in shear, the contact area, and thus the adhesive ability, greatly increases. C) The removal of the shear load allows the wedges to return to their default state, and allows easy release from the surface.

gripper with dry adhesives, (2) a model of the gripper on a variety of curvatures with varied initial conditions, (3) results verifying the model, showing self-engagement on textured glass, and demonstrating the implementation of the gripper onto a robotic arm, which can grasp objects that are ballistic or at rest, and (4) conclusions and future work.

## II. DESIGN

The shear adhesion gripper has two main components: the thin film with opposed gecko-inspired adhesives and the bi-stable support structure.

### A. Opposed Thin Film Gecko-inspired Adhesives

At the heart of the gripper is a set of opposed gecko-inspired adhesives, each cast directly onto a thin film of Kapton. The adhesive is polydimethylsiloxane (PDMS) microwedges [15], which have a property known as *controllability*. Controllability means that the adhesive increases contact area with the surface, causing additional adhesion as shear loads increase. When unloaded in shear, the contact area decreases. Therefore, in order to grasp an object, the pair of opposed adhesives need only be laid on the surface (at which point just the very compliant tip of each wedge engages with the surface) and loaded; there is no need to press them into the surface. Further, to release the grasp, the opposed adhesives are unloaded (Fig. 2) and lifted from the surface with a negligible force. After loading with 40 N, the release force was measured as less than 0.01 N, equivalent to less than 1/4000 of the loaded force.

1) *Thin Film Adhesive on Textured Surfaces*: If the surface is textured, only a small percentage of an adhesive will engage upon initial contact (Fig. 3a). For an adhesive to totally engage upon initial contact, either the film would need to stretch to match the curvature or the adhesive initially in contact would have to compress in the normal direction. In either case, a compressive preload would be required. However, angled fibers give an alternative: because the fibers initially in contact pull the backing closer to the surface during loading, the number of fibers in contact actually *increases* during loading (Fig. 3b-c) without ever being pressed into the surface. This is crucial for use of the gripper on textured surfaces; with even a small amount of initial

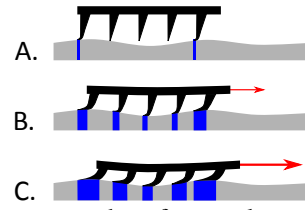


Fig. 3: A) On a textured surface, only a small percentage of the adhesive will be in contact initially. B) When loaded, however, the in-contact wedges will pull the backing closer to the surface, allowing other wedges to engage. C) Continued loading further increases contact area.

contact, the gripper can resist large forces. This effect is explored further in Sec. IV-B.

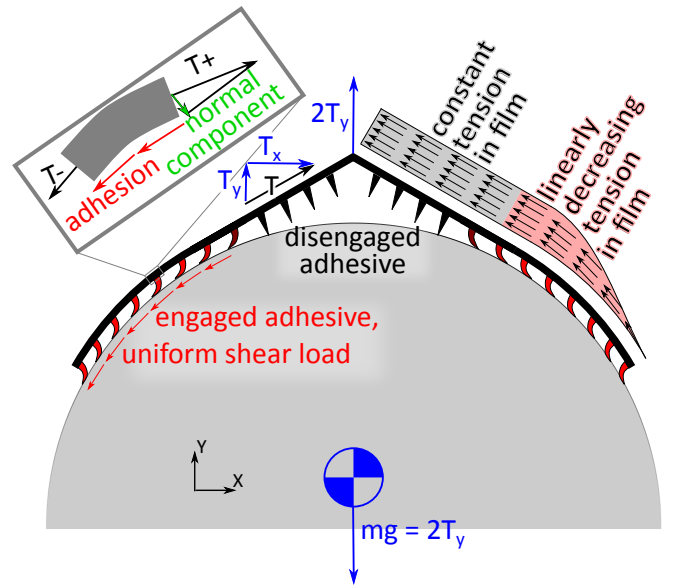


Fig. 4: The key forces acting on the gripper. The Y-component of the tension in the film is equal and opposite to one half of the weight of the object, while the X-component is cancelled internally. The tension is constant in the length of the film where the adhesives are disengaged but linearly decreases to zero in the region with adhesion. The adhesion is roughly constant across the length of the contact patch. Finally, when a small section of the engaged film is examined,  $T_+$ , in the direction towards the center of the gripper, is slightly larger than  $T_-$ . Both have a small normal component that faces toward the center of the object, which helps to pull non-engaged sections of the adhesive into contact.

2) *Forces in the Film*: The opposed adhesives from the two sides of the gripper apply two shear forces on the object, each directed along a tangent of the object toward the center of the gripper (Fig. 4), passing through the disengaged section of the film. Because microwedge adhesives can support much more load in shear than in the normal direction, this configuration, which does not depend on normal adhesion, exploits the strength of the shear adhesion.



Fig. 5: When the gripper is used to grasp a flat-sided object, the film is straight. In this case there are no forces due to the curvature of the film, yet the gripper still holds the object.

The Y-components of each of these two tensions developed from shear are the forces that support a grasped object. The X-components cancel one another internally.

The tension in the film in the center region that is not in contact with the object is uniform. However, in the region where adhesives are engaged with the surface, the tension is linearly decreasing, assuming that the adhesion is constant along the length of the engaged region. This assumption is based on a non-stretchable film, which is an approximation. In reality, because the film stretches slightly, there will be slightly more adhesion near the center of the gripper than at the tips. However, because the tension at the tip must be zero, if the stretch is small (causing a nearly-linear change in tension), the tension at any location along the film is known.

The forces that result from the film under tension on a curved surface are also important. If a small section of the film is examined, the tensions on either end do not oppose one another. Rather, both are directed slightly toward the object's center and thus have normal components. The magnitude of the normal force is much smaller than that of the shear force; for a 30 cm radius of curvature, the normal force is less than 3% of the shear force. Therefore, the effect of pushing away the object is very small. Further, there is a secondary, beneficial effect: if any small section of the film is not in contact in the engaged region, the normal force will press the adhesive into engagement. It is interesting to note, however, that these normal forces are not necessary for grasping. The gripper readily picks up an object with flat sides (Fig. 5).

### B. Bi-stable Support Structure

The second main component of the shear adhesion gripper is the bi-stable support structure. It is crucial that the film is laid onto the surface with minimal wrinkling (which decreases contact area and thus adhesion), so initiating a grasp with taut film is desirable. It is also important that the film conforms to the curved surface during the grasp. To achieve both of these design requirements, a support

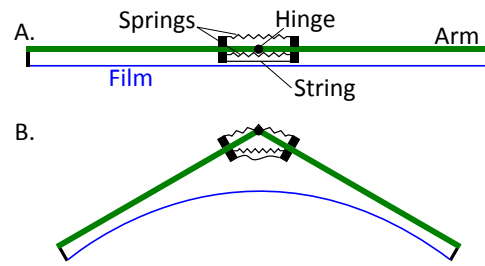


Fig. 6: A) Bi-stable support structure in the open state; the film is stretched taut. The top spring has a much larger moment arm than the bottom spring, resulting in the arms being pulled up. Once taut, the string on the bottom prevents the arms from being pulled further up. B) Structure in the collapsed state. Here, the film is allowed to curve around an object. The bottom spring now has a larger moment arm than the top spring, making the structure stable in the collapsed state.

structure was designed to be stable in both a straight position (allowing the film to be pulled taut), and in a collapsed position (allowing the film to conform to a curved surface) (Fig. 6).

The straight position (Fig. 6a) is stable because it is a local energy minimum; a small motion of the arms down increases the length of the top spring more than it decreases the length of the bottom spring, because their moment arms differ. A small motion of the arms up stretches the very stiff string, and also increases the systems energy. Similarly, the collapsed state is stable (Fig. 6b) because a motion of the arms up stretches the bottom spring more than the top one, and a motion of the arms down stretches the top spring while causing the bottom string to go slack.

### C. Using the Shear Gripper

To pick up a curved object, the gripper is first brought into contact with the object and has force applied to both arms to collapse the support structure (7b). Once the structure has collapsed and the film has come into contact with the surface, the gripper can be loaded to lift the object (7c). After manipulation is complete, the gripper can be released by lifting the two arms to return the gripper to its initial, straight configuration (7d).

Adding a plate, two pieces of foam, and “tails” on the ends of the arms enables the gripper to release without external actuation (Fig. 8). During contact with the object, the foam gently presses on the extents of the arms, causing the support structure to collapse. Loading occurs without interference from the foam. To release, the object is set down, and the rigid plate is pressed into the tails of the arms while the soft foam compresses. This action causes the support to become straight again, resetting the bi-stable structure, and releasing the object. The foam used is viscoelastic and remains compressed long enough to allow the pressing force to be removed. Elastic foam would recollapse the support structure while the pressing force was being removed.

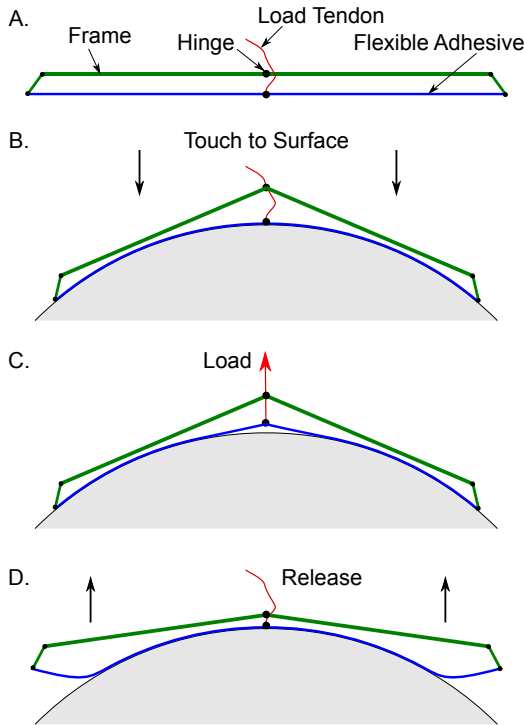


Fig. 7: A) The shear force gripper. B) To grasp an object, the arms of the gripper are pressed toward the object to collapse the structure and allow the film to contact the surface. C) The Load Tendon can then be pulled, lifting the object. D) To release, the arms are lifted to return the gripper to its initial state.

### III. MODEL

In order to predict the behavior of the gripper on various curvatures, a simple geometric model was developed.

#### A. Assumptions

The model assumes the object has a constant curvature and an evenly distributed mass: the object is symmetrically located below the gripper when hanging. Multiple curvatures will be explored in Section III-C. The model also assumes that the gripper is only using shear adhesion to hold the object, and thus the film extends away from the surface of the object along a tangent. In reality, there is a very small amount of normal adhesion at the peel zone of the film, applying a small amount of curvature to the film where it leaves the object's surface. However, this force is very small, measured as less than 0.25 N. There is also a small amount of normal pressure due to the tension in a curved film (See Sec. II-A.2), but it is estimated to be only a few percent of the tension. The surface of the object is also assumed to be of a uniform material and texture over the areas in which the gripper is in contact. Finally, the film is modeled as inextensible, while in reality it stretches less than one percent at the given loads.

#### B. Geometric Model

The model is based on the geometry shown in Fig. 9 (assuming the gripper is symmetric about the vertical axis),

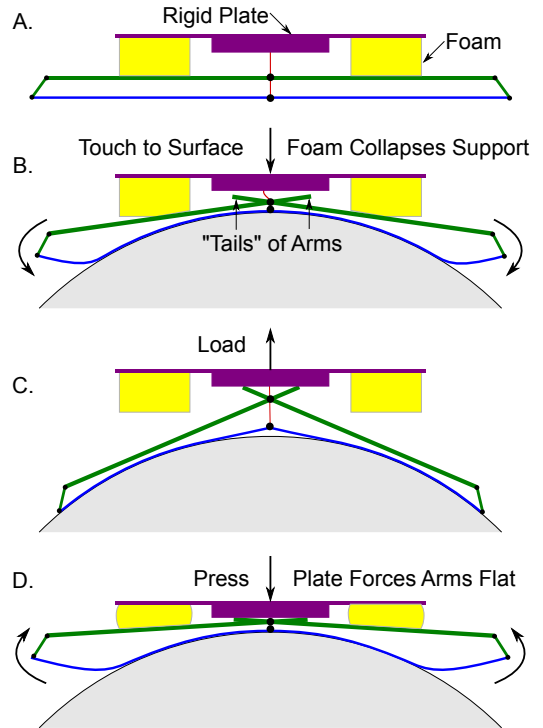


Fig. 8: A) In order to allow release without an actuator, another layer with compliance is added. B) To grasp an object, the gripper is brought into light contact, at which point the foam presses the arm to collapse the structure. C) Lifting the plate tension the Load Tendon and holds the object. D) To release, the object is pressed onto a surface, at which point the rigid plate presses the tails of the arms, returning the structure to its straight, initial position.

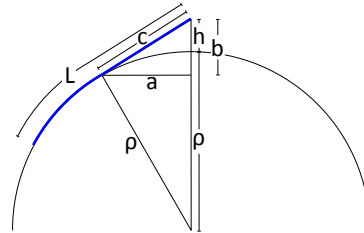


Fig. 9: The geometry on which the model is based.

where  $\rho$  is the radius of the object,  $h$  is the distance in the vertical direction from the object to the apex of the gripper (where the two films meet),  $b$  is the vertical distance from the point where the tangent leaves the surface to the apex of the gripper,  $c$  is the distance from the point where the tangent leaves the surface to the gripper's apex, and  $L$  is the film's length.

If the adhesive stress capability per unit length of film is  $P$ , then the force,  $F$ , that the gripper can provide to the object in the vertical direction is twice (one for each side) the vertical component of tension of the film; this tension is equal to  $P$  times the length in contact (Eq. 1).

$$F = 2P(L - c)\frac{b}{c} \quad (1)$$

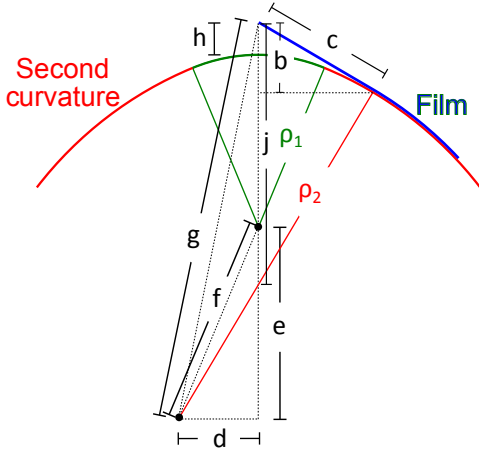


Fig. 10: The geometry on which the compound model is based.

To find  $F$ , the ratio of  $b$  to  $c$  must be determined, given  $\rho$ ,  $h$ , and  $L$ . By similarity, the ratio of  $b$  to  $c$  is equivalent to the ratio of  $c$  to  $(\rho + h)$ , thus only  $c$  must be found:

$$c = \sqrt{(\rho + h)^2 - \rho^2}. \quad (2)$$

### C. Compound Curvatures

The model was expanded to objects with two curvatures because many objects have two surfaces with large radii of curvature joined by a region of smaller radius of curvature (e.g. rounded corners). Fig. 10 shows the variables used in the compound curvature model.  $\rho_1$  is the radius of curvature of the middle section, while  $\rho_2$  is the radius of curvature of the two lateral regions.  $d$  is the horizontal distance from the center of the righthand lateral region,  $e$  is the vertical distance from the center of middle section to the center of the lateral section, and  $f$  is the hypotenuse of the triangle with sides  $d$  and  $e$ .  $g$  is the distance from the apex of the film to center of the lateral region, and  $j$  is the distance from the apex of the gripper to the point where the line from the center of the lateral region to the point where the film leaves the surface crosses the centerline.

The model is piece-wise with two cases. If the film is in contact with the middle region, the simple model above applies. However, if the film is not in contact with the middle region, then in order to calculate  $F$  from Eq. 1, different geometry must be used to find  $b$  and  $c$ . The angle between  $e$  and  $f$  is known from the geometry of the curves, and  $f$  is the difference between  $\rho_1$  and  $\rho_2$ . Thus  $e$  and  $f$  are easily calculated, allowing  $g$  be calculated as the hypotenuse of the triangle with  $d$  as its base. With  $g$ ,  $c$  can be calculated by the Pythagorean Theorem. The angle between the vertical and the line connecting the center of the lateral region and the point where the film leaves the surface is then known, so  $j$  can now be determined using  $c$ . By similar triangles, the ratio of  $b$  to  $c$  is then known, enabling the calculation of  $F$ .

With the model in hand, it is now possible to predict the maximum force that the gripper can sustain, given the size of the object, the shear ability of the adhesive on the object's

surface, and the height of the apex of the gripper above the surface. Further, since this final variable,  $h$ , can be set, it gives a degree of freedom for either designing a gripper for a particular curvature, or tuning an adjustable gripper for different curvatures.

## IV. RESULTS

Three main groups of tests were completed. First, the gripper was tested on a variety of curvatures, including one surface with compound curvature at different offset heights,  $h$ , to verify the model, and shows a maximum lifting ability of 43 N, or 13.5 kPa. Second, the thin film was loaded on a textured glass surface illuminated with Frustrated Total Internal Reflection (FTIR) to explore how the film interacts with such a surface. Third, the gripper was implemented onto an Adept robotic arm and made to grasp objects both ballistic and at rest.

### A. Model Verification

The first test completed to verify the model explored varying the radius of curvature of a surface while leaving the offset height constant. The second test varied the height offset while keeping the curvature constant. Finally, a compound curvature surface was tested at varying offsets.

1) *Methods:* For the first set of tests, a fixture was laser machined with slots at five different curvatures, and a 2 mm thick nylon sheet was fit into each slot. A pair of thin film adhesives (2.2 cm x 8 cm) was laid on the curved surface with a spacer to set the initial offset height and loaded slowly with a central tendon (approximately 3 N/s) until failure. The final offset height (which is slightly different than the initial offset due to film stretch) was recorded at 400 fps and analyzed after testing. The load was measured with a Mark-10 M4-50 digital pull-scale, with a 3kHz sampling rate and accuracy of 0.2% FS. 3 or 4 tests were performed for each test condition.

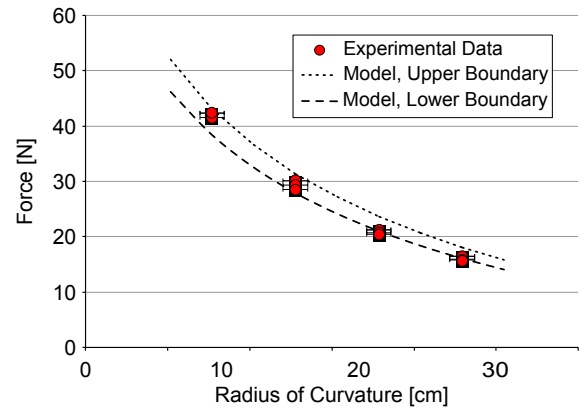


Fig. 11: Data showing maximum load capabilities of a gripper on surfaces of varying radii of curvature. The upper and lower bounds of the model are also shown. The estimated error in force is less than 0.5 N.

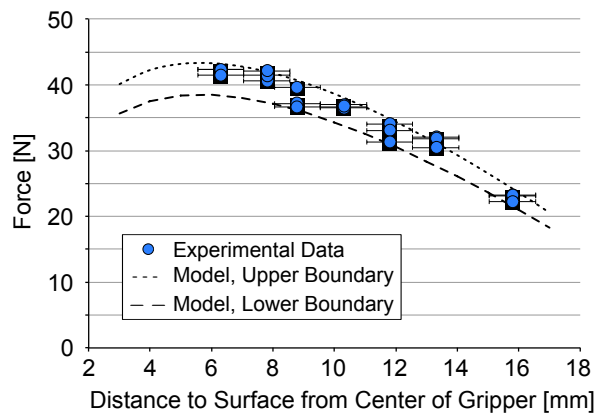


Fig. 12: Maximum load capabilities of a gripper on a surface while varying the height offset,  $h$ . The upper and lower bounds of the model are also shown.

2) *Varied Radius of Curvature*: The radius of curvature was varied from approximately 7 to 28 cm, with four radii tested. The results of the tests are shown in Fig. 11. The upper and lower boundaries of the model are shown as well; these correspond to the outputs of the model given the same geometry, but with the upper and lower limits of the expected shear capabilities of the adhesive (the value of  $P$ ). In this range, the data and model both show that an increasing radius of curvature leads to a smaller maximum force capability. Because only shear adhesion is modeled, an asymptote exists at zero force, which is approached for infinite radius of curvature; in this condition, the ratio of  $b$  to  $c$  is zero. In reality there is a small amount of force capability due to non-zero normal adhesion. The model also predicts that the force continues to increase as the radius of curvature decreases; however this is inaccurate for very small radii of curvature, since the amount of surface available for adhesion begins to decrease.

3) *Varied Height Offset*: The height offset,  $h$ , was varied from approximately 6 to 16 mm. The results of the tests for varied  $h$  are shown in Fig. 12. The model and the data show a generally decreasing force ability with increasing  $h$ . However, the model shows a peak force ability near an  $h$  of 6 mm. The predicted force capability then decreases with smaller  $h$  values due to the fact that the ratio of  $b$  to  $c$  decreases faster than the contact area increases. Unfortunately, with the current film, it was infeasible to test  $h$  values lower than 6 mm, due to film stretch.

4) *Compound Curvature*: Again, the height offset,  $h$ , was varied, but now the surface had two distinct curvatures: the middle region a radius of curvature ( $\rho_1$ ) of approximately 12.5 cm and the two lateral sections a radius of curvature ( $\rho_2$ ) of 30 cm. The data and model are shown in Fig. 13. The non-smoothness in the first order can be seen, due to the piecewise nature of the model. The data also reflects this transition and shows a marked decrease in force ability once the film is only on the lateral regions; the dotted line shows the predicted performance for a surface with a single radius of curvature,  $\rho = 12.5$  cm.

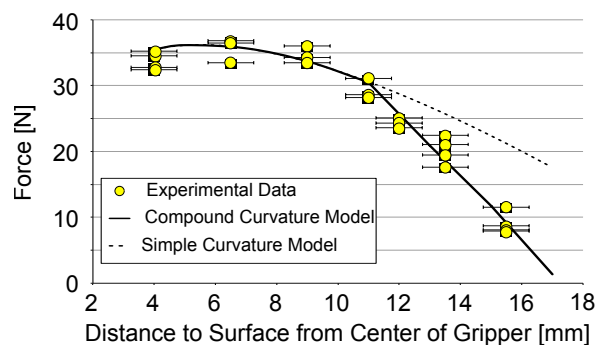


Fig. 13: Maximum load capabilities of a gripper on a surface with compound curvature while varying the height offset,  $h$ . The radius of curvature in the middle region is approximately 12.5 cm, and in the lateral region, 30 cm. The model is also shown (note the model and data show a lower maximum than in previous plots, because a slightly different adhesive was used). The dotted line shows the predicted performance if the radius of curvature remained at 12.5 cm throughout the surface.

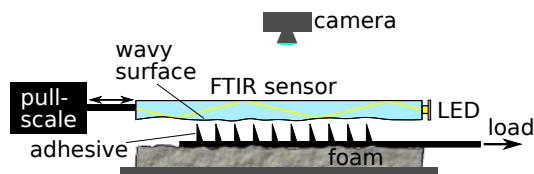


Fig. 14: Experimental setup for FTIR tests.

### B. Thin Film Adhesive on Textured Surface

To test whether the angled fibers that compose the adhesive allow the gripper to increase contact area as larger shear loads are applied, a textured surface was instrumented with FTIR.

1) *Methods*: A 10 cm x 10 cm x 2 mm plate of textured glass was lit with LEDs along one edge (Fig. 14). The glass was set face down on a piece of foam. Between the glass and the foam, a 2 cm x 3 cm section of thin film adhesive was placed, facing the glass, with a pull tab extending beyond the glass plate. The glass was affixed to a pull-scale on one end, and the adhesive film was pulled via the tab in the opposite direction. A video was captured in a dark room of the experiment at 60 fps, 1080p. Frames from the video were then run through a filter to convert to black and white, and the area of the white (lit or in contact) section was measured. Each frame was correlated to the load on the scale at the time of capture.

2) *FTIR Data*: Frustrated total internal reflection can be used to image the real area of contact of an adhesive against a glass surface. Two adhesive films were tested: PDMS microwedges as well as PDMS cast on a smooth glass surface, the latter acting as a control. The films were identical besides the presence of the wedges on the former. Representative frames from the tests are shown in Fig. 15. Fig. 16 shows data from the captured frames plotted as contact area versus load. Both representations of the data show that the flat PDMS film does not increase contact area with load. Without an

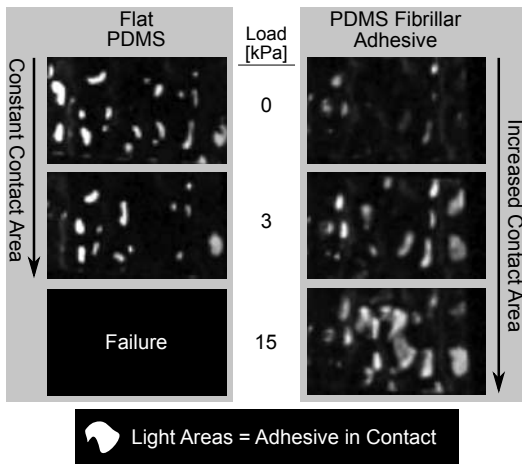


Fig. 15: Frames from the recording of FTIR tests. On the left, PDMS without features, on right PDMS with microwedges. Load increases in lower frames. Note that contact area increases with fibrillar film, allowing much larger load.

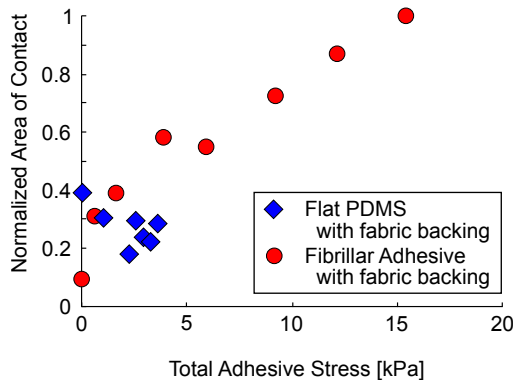


Fig. 16: Data from the FTIR recording showing contact area versus applied load. Blue diamonds represent flat PDMS, which does not show an increase in contact area with load. No increase in contact area means no increase in load ability. In contrast, the PDMS with microwedges, represented by red circles, shows a marked increase in contact area with load, resulting in a much higher load capability.

increase in contact area, the flat PDMS can only support a load equivalent to that allowed by initial contact area. PDMS textured with angled microwedges does show an increase in contact area with load. The increase in area allows a large increase in sustainable load, nearly 3 times larger than that of the flat PDMS. Further, because the default, zero-load state shows lower contact area (approximately 1/4 of flat PDMS), the film releases more easily when desired. The low default state contact area is due to only the tips of the microwedges touching the surface.

### C. Implementation onto a Robotic Arm

Because object contact is the sole requirement for the gripper to initiate grasping, the implementation onto an arm is very straightforward. Simply attaching the gripper, and adding a single servo for release is sufficient. However, it is also possible to use the gripper with no actuated degrees of



Fig. 17: Objects picked and placed by a robotic arm using the shear adhesion gripper. Clockwise, from upper left: packing tape, PVC tubing, 5 gallon water bottle, and basketball.



Fig. 18: Gripper catching a ballistic object. *Left*, The instant before contact is made ( $t = 0$ ). *Center*, The gripper collapses ( $t = 20$  ms). *Right*, The ball rebounds, but the adhesive has engaged, and the gripper has caught the ball ( $t = 88$  ms).

freedom if release is always done by setting an object down on a surface, using the design presented in Sec. II-C.

Four objects were placed within the workspace of an Adept 5-DOF arm, and subsequently picked, moved, and placed. The objects, as shown in Fig. 17, were a roll of packing tape, a 1.3 m long, 15 cm diameter piece of 6 mm wall thickness tubing, a regulation-size basketball, and an empty 5 gallon water bottle. The gripper is also able to grasp a Ziploc bag partially filled with water (Fig. 19). The heavy object (tube) shows its ability to carry over 3 kg. The large diameter objects (ball and bottle) exemplify how the gripper can work without needing to wrap far enough around an object to squeeze. Finally, the water bag displays an ability to grasp nonconventional objects.

Finally, a ball was tossed to the gripper, which caught it passively (Fig. 18). The adhesives are able to engage very rapidly, due to the small size of individual wedges. Engagement is limited by the speed at which PDMS can bond to the surface [16], the engagement required to catch the ball can be estimated to occur in 5 ms [17]. The device is passive, which adds to the ease of catching; no fast sensing



Fig. 19: Objects picked and placed by a robotic arm outfitted with the shear force gripper.

nor high power actuation is required. Finally, because of the very small mass of the gripper (less than 15 g), the whole gripper is allowed to accelerate with the object during rebound, tethered by a nearly constant-force spring [18]. This means required grasping forces are greatly reduced when compared to a rigid gripper.

## V. CONCLUSIONS AND FUTURE WORK

In this work, we presented a novel gripper which grasps objects utilizing shear forces derived from controllable fibrillar gecko-inspired adhesives cast directly onto a thin film. We introduced a model to determine the forces the gripper can apply to concave objects with up to two distinct curvatures and verified the model experimentally. We tested the adhesive-clad thin film on textured glass and observed its performance with FTIR; it shows a beneficial characteristic (increased engagement with load), which was not observed with flat PDMS. Finally, we implemented the gripper onto a robotic arm to grasp a variety of objects, including a tossed ball and a partially filled Ziploc bag.

These results show that a shear adhesion gripper is a viable option for robotic grasping of large radius of curvature objects. Further, when implemented with controllable fibrillar adhesives, the gripper can be functional on textured surfaces, can work in dynamic applications, and can easily release an object. Additionally, it can grasp very delicate objects, since it does not depend on squeezing, is light (weighs 0.015 kg but can lift 4.3 kg), is very low cost (less than 2 USD) and requires no actuation to close. With these characteristics, the gripper has possible applications in manufacturing, especially in automobile glass, lighting fixture, or tubing factories, as well as on low cost robotic arms.

Future work for the gripper includes developing a more general model for grasping any shape, and extending this model to three dimensions. For spherical objects, designing a gripper with three arms could provide advantages. Adding

stabilizing elements to lock an object once grasped is desirable; the current design allows the object to move relatively freely. Finally, reworking the manufacturing process to cast fibrillar adhesives directly onto a material that is stiffer in tension than Kapton could provide larger load capability by reducing film stretch.

## ACKNOWLEDGMENTS

EWB was supported by the NSF GRFP. DLC was supported by SRI and DARPA HR0011-12-C-0040.

## REFERENCES

- [1] M. Racic, "The belgrade hand prosthesis," *Proc. Instn. Mech. Engrs*, vol. 183, pp. 1968–69, 1969.
- [2] J. K. Salisbury and J. J. Craig, "Articulated hands force control and kinematic issues," *The International Journal of Robotics Research*, vol. 1, no. 1, pp. 4–17, 1982.
- [3] S. Jacobsen, E. Iversen, D. Knutti, R. Johnson, and K. Biggers, "Design of the utah/mit dextrous hand," in *Robotics and Automation. Proceedings. 1986 IEEE International Conference on*, vol. 3. IEEE, 1986, pp. 1520–1532.
- [4] M. Ciocarlie and P. Allen, "A constrained optimization framework for compliant underactuated grasping," *Mech. Sciences*, vol. 2, no. 1, pp. 17–26, 2011.
- [5] M. G. Catalano, G. Grioli, A. Serio, E. Farnioli, C. Piazza, and A. Bicchi, "Adaptive synergies for a humanoid robot hand," in *Humanoids*, 2012, pp. 7–14.
- [6] F. Lotti, P. Tiezzi, G. Vassura, L. Biagiotti, G. Palli, and C. Melchiorri, "Development of ub hand 3: Early results," in *Robotics and Automation, 2005. ICRA 2005. Proceedings of the 2005 IEEE International Conference on*. IEEE, 2005, pp. 4488–4493.
- [7] A. M. Dollar and R. D. Howe, "Joint coupling design of underactuated grippers," in *ASME 2006 International Design Engineering Technical Conferences and Computers and Information in Engineering Conference*. American Society of Mechanical Engineers, 2006, pp. 903–911.
- [8] L. U. Odhner, R. R. Ma, and A. M. Dollar, "Open-loop precision grasping with underactuated hands inspired by a human manipulation strategy," *Automation Science and Engineering, IEEE Transactions on*, vol. 10, no. 3, pp. 625–633, 2013.
- [9] D. Aukes, S. Kim, P. Garcia, A. Edsinger, and M. R. Cutkosky, "Selectively compliant underactuated hand for mobile manipulation," in *(ICRA), 2012 IEEE*. IEEE, 2012, pp. 2824–2829.
- [10] M. C. Carrozza, C. Suppo, F. Sebastiani, B. Massa, F. Vecchi, R. Lazzarini, M. R. Cutkosky, and P. Dario, "The spring hand: development of a self-adaptive prosthesis for restoring natural grasping," *Autonomous Robots*, vol. 16, no. 2, pp. 125–141, 2004.
- [11] C. Melchiorri and M. Kaneko, "Robot hands," *Springer Handbook of Robotics*, pp. 345–360, 2008.
- [12] D. Prattichizzo and J. C. Trinkle, "Grasping," *Springer handbook of robotics*, pp. 671–700, 2008.
- [13] E. Brown, N. Rodenberg, J. Amend, A. Mozeika, E. Steltz, M. R. Zakin, H. Lipson, and H. M. Jaeger, "Universal robotic gripper based on the jamming of granular material," *Proceedings of the National Academy of Sciences*, vol. 107, no. 44, pp. 18 809–18 814, 2010.
- [14] S. Song, C. Majidi, and M. Sitti, "Geckogripper: A soft, inflatable robotic gripper using gecko-inspired elastomer micro-fiber adhesives," in *Intelligent Robots and Systems (IROS), 2013 IEEE/RSJ International Conference on*. IEEE, 2014, pp. 4624–4629.
- [15] P. Day, E. V. Eason, N. Esparza, D. Christensen, and M. Cutkosky, "Microwedge machining for the manufacture of directional dry adhesives," *J Micro and Nano-Man.*, vol. 1, no. 1, p. 011001, 2013.
- [16] B.-m. Z. Newby and M. K. Chaudhury, "Friction in adhesion," *Langmuir*, vol. 14, pp. 4865–4872, 1998.
- [17] D. Christensen, E. W. Hawkes, A. Suresh, and M. Cutkosky, "utugs: Enabling microrobots to deliver macro forces with controllable, bio-inspired adhesives," in *International Conference on Robotics and Automation*, 2014, submitted.
- [18] E. W. Hawkes, D. L. Christensen, E. V. Eason, M. A. Estrada, M. Heverly, E. Hilgemann, H. Jiang, M. T. Pope, A. Parness, and M. R. Cutkosky, "Dynamic surface grasping with directional adhesion," in *Intelligent Robots and Systems (IROS), 2013 IEEE/RSJ International Conference on*. IEEE, 2013, pp. 5487–5493.